Elongation of very long chain fatty acids protein 7 (ELOVL7)

A Target Enabling Package (TEP)

Gene ID / UniProt ID / EC	**79993** / **A1L3X0** / **EC 2.3.1.199**
Target Nominator	SGC Internal Nomination
SGC Authors	Laiyin Nie[1], Ashley C.W. Pike[1], Tomas C. Pascoa[1], Shubhashish M.M. Mukhopadhyay[1], James D. Love[2], Nicola A. Burgess-Brown[1], Paul E. Brennan[1], Elisabeth P. Carpenter[1]
Target PI	Liz Carpenter (SGC Oxford)
Therapeutic Area(s)	Metabolic diseases
Disease Relevance	A variety of inherited diseases are caused by mutations in genes encoding very long chain fatty acid (VLCFA)-metabolising enzymes including the ELOVL elongases. ELOVL elongases are potential therapeutic targets for conditions in which VLCFAs accumulate such as X-linked adrenoleukodystrophy.
Date Approved by TEP Evaluation Group	27th November 2020
Document version	1.0
Document version date	November 2020
Citation	Laiyin Nie, Ashley C.W. Pike, Tomas C. Pascoa, Shubhashish M.M. Mukhopadhyay, James D. Love, Nicola A. Burgess-Brown, … Elisabeth P. Carpenter. (2020). Elongation of very long chain fatty acids protein 7 (ELOVL7); A Target Enabling Package [Data set]. Zenodo. http://doi.org/10.5281/zenodo.4428940
Affiliations	1. Centre for Medicines Discovery, Old Road Campus Research Building, Headington, Oxford OX3 7DQ, UK. 2. Albert Einstein College of Medicine, Department of Biochemistry, New York, NY 10461-1602, USA

USEFUL LINKS

(Please note that the inclusion of links to external sites should not be taken as an endorsement of that site by the SGC in any way)

SUMMARY OF PROJECT

The long-chain fatty acid elongases (ELOVL) catalyse the first rate-limiting step in the two carbon elongation of the acyl chains of fatty acids (FAs) greater than 12 carbons in length (1). Defects in these ELOVL elongases cause severe genetic diseases, such as Stargardt disease-3 and several ataxias, and knockout studies suggest roles in insulin resistance and hepatic steatosis (2). This TEP provides the first structural information for this family of enzymes which, coupled with mutagenesis and biophysical studies, demonstrates how substrates and products bind within the active site.

SCIENTIFIC BACKGROUND

Long chain FAs (LCFA; 12-20 carbons in length) and very long chain FAs (VLCFA; more than 20 carbons) are the precursors for synthesis of ceramides, sphingolipids and sphingolipid signalling molecules. Sphingolipids derived from VLCFAs are essential for membrane stability and play important roles in the myelin sheaths of nerves, formation of the skin permeability barrier, and in brain, retina and liver function (2).

FAs up to 16 carbons in length are synthesised by the well-characterised fatty acid synthase system. Longer FAs are either obtained from the diet or produced in the endoplasmic reticulum (ER) by the FA elongation cycle (2,3), which comprises four distinct membrane-embedded enzymes that perform sequential reactions to extend the acyl chain of fatty acids by two carbon units per cycle (**Fig 1**). The first rate-limiting step of this cycle is a condensation reaction between an acyl-CoA and malonyl-CoA (the two-carbon donor) to form a 3-keto acyl-CoA. This initial reaction is catalysed by the long-chain fatty acid elongases (ELOVLs) (also known as 3-keto acyl-CoA synthases).

In humans, there are seven ELOVL enzymes (ELOVL1-7), sharing 24-57 % sequence identity, which have different acyl-CoA substrate specificities with distinct preferences for acyl chain length and degrees of FA unsaturation (3,4). The 3-keto acyl-CoA product of this first reaction is further processed by the other three ER-resident enzymes in the cycle (**Fig 1A**) resulting in an acyl-CoA that can be further extended up to a maximum chain length of about ca. 38 carbons. ELOVL7 elongates C16-C20 acyl-CoAs with higher activity towards C18 acyl-CoAs, in particular C18:3(n-3) and C18:3(n-6) acyl-CoAs (5).
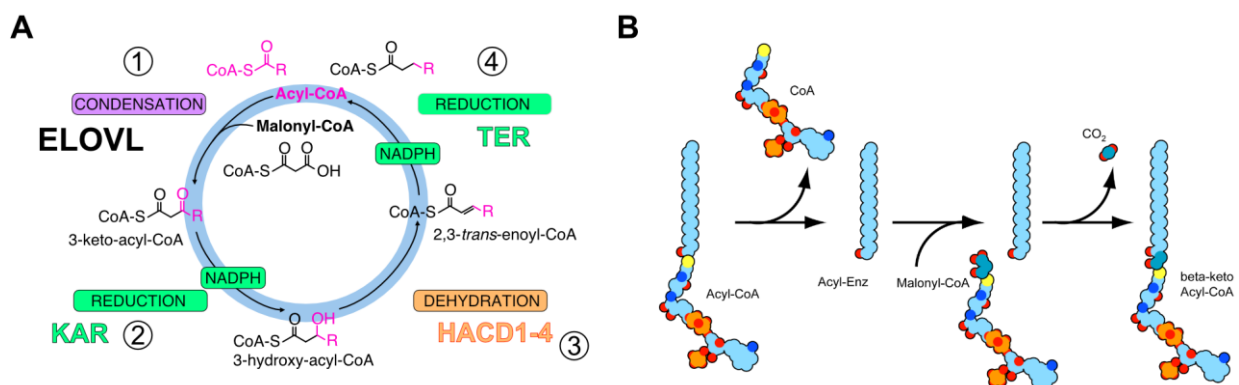

Figure 1. (A) Fatty acid elongation cycle. The cycle comprises four ER-resident integral membrane enzymes - an elongase (ELOVL), 3-keto acyl-CoA reductase (KAR), 3-hydroxy acyl-CoA dehydratases and trans-2,3-enoyl-CoA reductase (TER) - carry out sequential reactions that extends the acyl chain. (B) Schematic representation of ELOVL catalysed condensation reaction.

Defects in FA elongation have serious downstream effects for lipid synthesis and function. Mutations in the *ELOVL4* gene cause Stargardt disease-3 (juvenile macular degeneration), ichthyosis (skin condition), intellectual disability, spastic quadriplegia and spinocerebellar ataxia 34 (SCA34) (6). *ELOVL5* mutations cause spinocerebellar ataxia 38 (SCA38) (7). *Elovl3* knockout mice suffer severely from hair loss and have an imbalance in the lipid species of the sebum (8); and mouse knockout studies of *elovl5* and *elovl6* suggest associations with hepatic steatosis and obesity-induced insulin resistance (9,10). ELOVL7, the most recently discovered member of the family , is associated with prostate (11,12), gynaecological cancer and early onset Parkinson's disease (13). ELOVL7 knockdown reduces cell death and membrane permeabilization during necroptosis, a form of programmed cell death (14).

ELOVL elongases are potential therapeutic targets for conditions arising from the accumulation of VLCFAs. For example, in X-linked adrenoleukodystrophy (X-ALD) defects in the transporter that targets VLCFAs for degradation in the peroxisomes results in the build-up of C24 and C26 VLCFAs in plasma and tissues. Increased levels of VLCFA-CoAs are substrates for further elongation. Modulation of ELOVL1 activity, the

isoenzyme mainly responsible for production of saturated C26:0 VLCFAs, may help to reduce synthesis of this fatty acid, and counteract its harmful effects in X-ALD (15).

Understanding the structure-function relationship of the family of ELOVLs is key for advancing target and therapeutic discovery. To date, however, very little is known about the molecular mechanisms underlying this key step in FA synthesis by the ELOVLs. In this TEP, we have developed methods for protein expression and purification of ELOVL7 as well as solving its structure in complex with a fortuitously-bound, co-purified product analogue. Our data allow us to begin to understand how substrates and products bind to the enzyme and provides insights into the elongation reaction mechanism.

RESULTS – THE TEP

Proteins purified

Human ELOVL7 is 281 amino acids in length and predicted to have seven transmembrane (TM) segments. We have expressed full-length ELOVL7 with a C-terminal TEV-10His-Flag tag in both insect (*Sf9*) and mammalian (Expi293F) cells. ELOVL7 is purified in octyl glucose neopentyl glycol (OGNG) supplemented with cholesteryl hemisuccinate (CHS) and can be concentrated to 10-25 mg/ml in this detergent/lipid combination. Heterologously-expressed ELOVL7 is a mixture of unmodified WT protein and protein covalently-bound to a 3-keto acyl-CoA (+1074Da mass adduct), as revealed by intact mass spectrometry (see **Fig 3C** in next section). The covalently modified species is more stable as it represents over 90% of the final purified protein.

Structural data

We have crystallised and solved the structure of ELOVL7 to a resolution of 2.6 Å [PDB: **6Y7F**]. Overall ELOVL7 has seven TM helices (TM1-TM7) which adopt a novel fold with TM2-7 forming a six TM inverted barrel surrounding a narrow tunnel (**Fig 2**). Each side of the barrel is formed by three helices (TM2-4 and TM5-7) that are arranged in an antiparallel fashion (**Fig 2C, D**). These two helical units are assembled as an inverted repeat around the central tunnel with TM1 lying against TM3/4, outside the barrel. ELOVL7 crystallises as a head-to-tail dimer (**Fig 2E**). This arrangement is consistent with size-exclusion chromatography with multi-angle light scattering (SEC-MALS) analysis in solution. The dimer interface has a small and unconserved interaction surface.
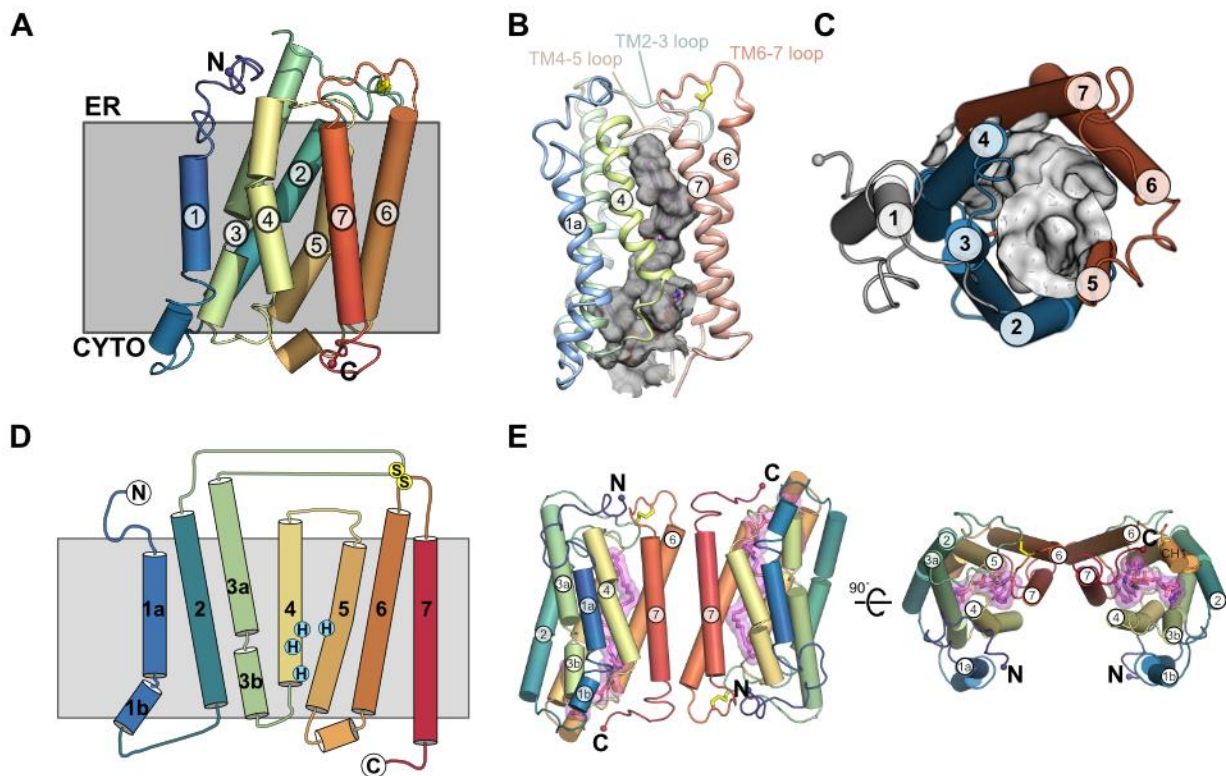
Figure 2. (A) Structure of human ELOVL7 [PDB: 6Y7F]. **(B)** Molecular surface representation of the central tunnel running the entire length of the protein. **(C)** Inverted barrel topology. TM helices 2-4 (blue) and 5-7 (orange) form either side of the barrel that surrounds the central tunnel. **(D)** TM helix topology. The locations of the disulphide bridge (S-S) connecting the TM2/3 and TM6/7 loops and the conserved active site histidines (H) are highlighted. **(E)** ELOVL head-to-tail dimer arrangement in the crystal. The bound product (magenta) is shown in stick and surface representation.

The central tunnel is 35 Å long and has a narrow (8-10 Å wide) opening on the cytoplasmic face of the protein (**Fig 2B**). The tunnel spans the entire membrane bilayer and is sealed at its ER lumen end by the short membrane-embedded loop between TM4-5, which connects the two halves of the barrel. The structure revealed that a covalently-bound product analogue had copurified with the enzyme (**Fig 3**). This C20 3-keto acyl-CoA spans the entire length of the tunnel with the CoA portion bound at the cytoplasmic entrance and the acyl chain is buried at the occluded ER end of the tunnel (**Fig 3B**). The acyl chain binding pocket is kinked presumably allowing unsaturated acyl-CoAs to bind.

The active site lies at the midway point of the membrane and includes the conserved canonical ELOVL [147]HxxHH[151] 'histidine-box' sequence. The 3-keto acyl-CoA is covalently bound to two histidines (H150 & H181) within the active site (**Fig 3B,** *inset*). His150 is the second histidine in the HxxHH motif on TM4 and His181 is located on TM5 in another conserved cluster of residues that have been shown to be critical for elongase function (16).
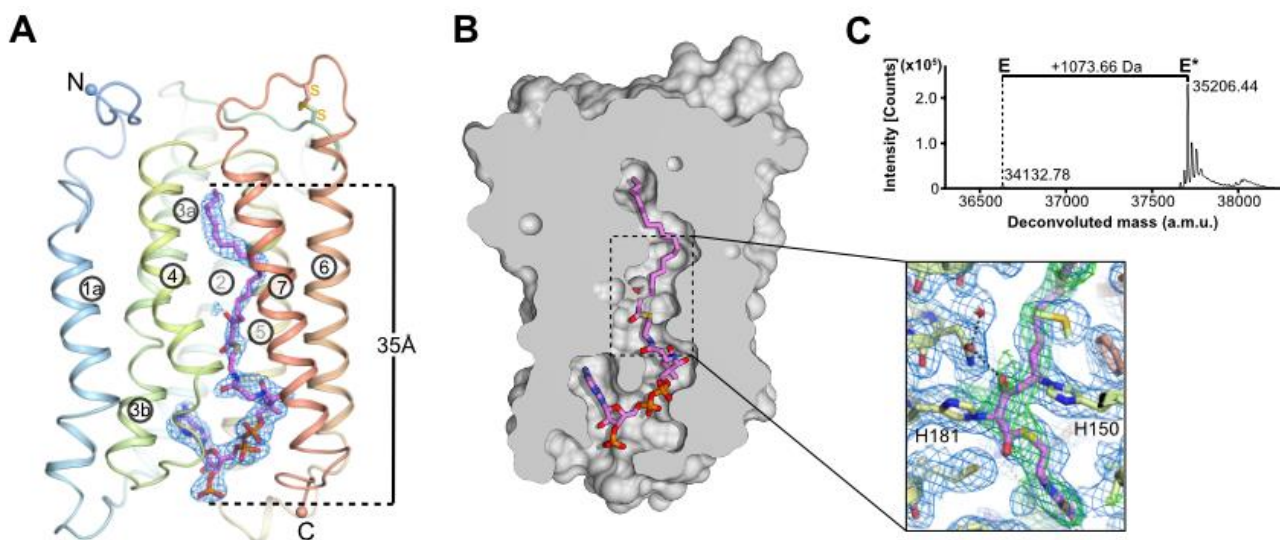
Figure 3. (A) Electron density for covalently bound acyl-CoA [PDB: 6Y7F]. **(B)** Sliced molecular surface view highlighting extent on central active site tunnel and (inset) electron density for acyl-CoA covalently bound to active site histidines. The refined 2mFo-DFc (blue mesh, contoured at 1 sigma) and omit mFo-DFc (green mesh, contoured at 2.5 sigma) electron density maps are shown overlaid on the final model. **(C)** Denaturing intact mass spectrometry analysis of purified protein shows that the modified enzyme (E*) represents the major species after SEC purification.

The structure suggests that the ELOVL elongation reaction most likely proceeds via a ping-pong type, two-step mechanism (**Fig 4A**) as the active site tunnel is too narrow to accommodate both acyl-CoA substrates simultaneously. In the first transacylation step, the acyl-CoA binds and its acyl chain is transferred to His150 via a C-N linkage resulting in an acyl-imidazole intermediate (**Fig 4C**, *left*). The CoA portion can then dissociate prior to the binding of the second substrate, the two-carbon donor malonyl-CoA (**Fig 4C**, *middle*). We hypothesise that in the second condensation step, malonyl-CoA undergoes decarboxylation to provide a nucleophilic enolate that can then react with the acyl-enzyme intermediate to produce the final product (**Fig 4C**, *right*). We have been able to detect the formation of an acyl-enzyme intermediate on incubation with the first acyl-CoA substrate via mass spectrometry (see next section).
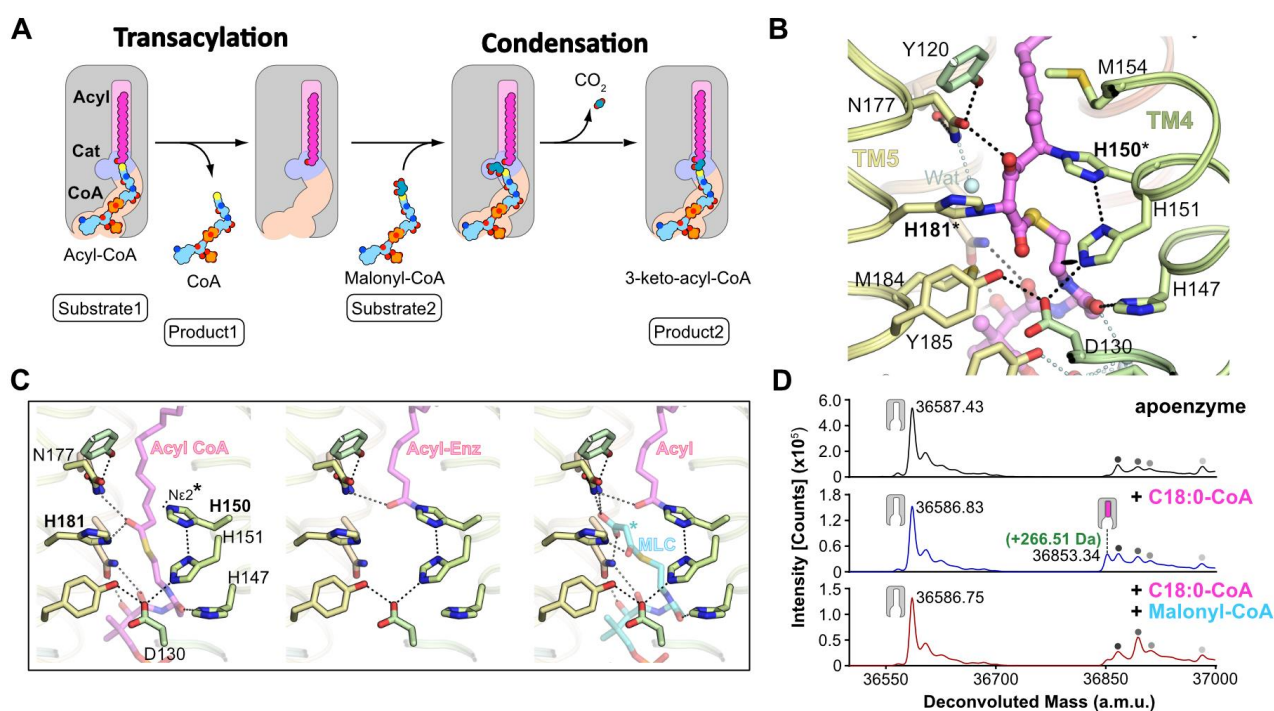
Figure 4 (A) Proposed ELOVL ping-pong type reaction mechanism. **(B)** View of active site around conserved HxxHH motif [PDB: 6Y7F]. **(C)** Structural models for steps in catalysis - (*left-to-right*) acyl-CoA binding, acyl-enzyme formation and malonyl-CoA (MLC) binding prior to decarboxylation and product formation. **(D)** Detection of an acyl-enzyme intermediate using mass spectrometry. Enzyme was incubated with either first substrate (middle; C18:0-CoA) or both substrates (bottom; C18:0-CoA & malonyl-CoA). Incubation with substrate produced a new species consistent with an acyl-enzyme intermediate (+266.5Da) (black/grey circles indicate background species present in starting apoenzyme sample).

Assays

We monitored the ELOVL7 reaction using intact mass spectrometry and demonstrated that FA chain elongation by ELOVLs proceeds via a stable acyl-imidazole intermediate (**Fig 4D**). We monitored acyl-enzyme formation using the small proportion of active, unmodified protein. Incubation of the enzyme with the first substrate C18:0 acyl-CoA gave rise to an additional peak, compared to the apo-enzyme, corresponding to an enzyme adduct with the expected mass addition for the C18:0 acyl chain (+266.47 Da) (**Fig 4D**, *top & middle*). Incubation with both substrates (C18:0 acyl-CoA and malonyl-CoA) greatly reduced accumulation of the adduct intermediate, consistent with the reaction having gone to completion (**Fig 4D**, *bottom*). The formation of this intermediate is not affected by either EDTA or EGTA (data not shown; see ref (17)) suggesting that, despite the large number of histidines in the active site, the elongation reaction does not appear to be zinc/metal-dependent. No adduct formation was observed on incubation of a His150Ala mutant with C18:0 acyl-CoA demonstrating that the second histidine in the conserved Hxx**H**H ELOVL histidine box is the site of transacylation.

Chemical Matter

The structure reveals the identity of the 1074Da adduct observed in MS analysis. We have modelled a 3-keto eicosanoyl (C20)-CoA (**Fig 5,** *product 2*) bound via its C2 and C5 carbons to His181 and His150 respectively (**Fig 4B**). We hypothesise that the observed adduct is formed when heterologously expressed material reacts irreversibly *in vivo* to form a dead-end complex with a *trans*-enoyl-CoA formed either as an intermediate in the elongation cycle or due to VLCFA degradation.
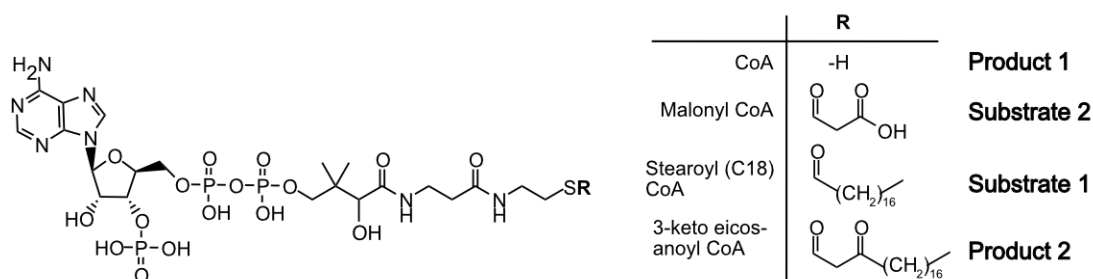

Figure 5 Chemical structure of examples of ELOVL7's acyl-CoA substrates and products.

IMPORTANT: Please note that the existence of small molecules within this TEP indicates only that chemical matter might bind to the protein in potentially functionally relevant locations. The small molecule ligands are intended to be used as the basis for future chemistry optimisation to increase potency and selectivity and yield a chemical probe or lead series. As such, the molecules within this TEP should not be used as tools for functional studies of the protein, unless otherwise stated, as they are not sufficiently potent or well-characterised to be used in cellular studies.

CONCLUSION

The acyl-CoA-bound crystal structure of ELOVL7 presented in this TEP represents the first example for the elongase family and provides the foundation for understanding the molecular basis of this key step in FA synthesis. The unusual architecture, active site arrangement and chemistry revealed by our structure provides exciting new avenues for design of modulators of ELOVL activity. Such compounds may be

beneficial in the treatment of patients with X-linked adrenoleukodystrophy (X-ALD), an inherited metabolic disorder in which patients are unable to breakdown VLCFAs due to defects in the peroxisomal FA degradation pathway. VLCFA accumulation leads to demyelination and damage to the adrenal cortex resulting in adrenocortical insufficiency and progressive loss of physical and mental function. Knockdown of ELOVL1, which is responsible for the production of C24-C26 VLCFAs that accumulate in X-ALD patients, partially restores the FA profile in X-ALD patient-derived fibroblasts (15). Furthermore, Lorenzo's oil, a dietary treatment for X-ALD patients (18), has effects on the activity (19) and expression of several ELOVLs (20). The design of specific ELOVL elongase inhibitors may offer a route to reduction of accumulating VLCFAs, thus providing a novel approach to therapy for this devastating disease.

Next steps
- Structural studies of the apo-enzyme / mutants with defined substrates are planned to further understand the elongation mechanism. Apo-enzyme will require stabilization, possibly through addition of substrates, such as malonyl-CoA, during purification. Mutants of His150/181, as well as at residues in the putative decarboxylation pocket, also warrant further structural characterization.
- Further assay development to allow product quantitation using intact mass spectrometry, similar to that described in (21), will allow monitoring of the full elongation reaction and enable us to characterise experimental and disease variants.

TEP IMPACT

Publications arising from this work:
This work has been written up for publication and is available as a preprint Nie *et al.* (2020) (17).

FUNDING INFORMATION

ADDITIONAL INFORMATION

Structure Files

PDB ID	Structure Details
6Y7F	ELOVL7 crystal structure with covalently bound 3-keto-eicosanoyl-CoA

Materials and Methods

Protein Expression and Purification
Vector: pFB-CT10HF-LIC (available from The Addgene Nonprofit Plasmid Repository)

Cell line: DH10Bac, Sf9 cells, Expi293F

Tags and additions: C-terminal TEV protease site, followed by 10x His and FLAG tags

Construct sequence: Residues 1 – 281

MAFSDLTSRTVHLYDNWIKDADPRVEDWLLMSSPLPQTILLGFYVYFVTSLGPKLMENRKPFELKKAMITYNFFIVLFSVYMC
YEFVMSGWGIGYSFRCDIVDYSRSPTALRMARTCWLYYFSKFIELLDTIFFVLRKKNSQVTFLHVFHHTIMPWTWWFGVKFA
AGGLGTFHALLNTAVHVVMYSYYGLSALGPAYQKYLWWKKYLTSLQLVQFVIVAIHISQFFFMEDCKYQFPVFACIIMSYSF
MFLLLFLHFWYRAYTKGQRLPKTVKNGTCKNKDNAENLYFQSHHHHHHHHHHHDYKDDDDK

(underlined sequence contains vector encoded TEV protease cleavage site, His and FLAG tag)

The human ELOVL7 gene (HGNC:26292; Gene ID 6505), which encodes the ELOVL7 protein (ELOVL fatty acid elongase 7; residues Met1 to Asn281), was subcloned into the pFB-CT10HF-LIC vector and baculovirus was generated using the Bac-to-Bac system. Briefly, this was performed by transforming into the *Escherichia co*li strain DH10Bac, to generate bacmid DNA, which was then used to transfect *Spodoptera frugiperda* (Sf9) insect cells, from which recombinant baculovirus were obtained. Large scale grow-ups of Sf9 cells were infected with baculovirus and incubated for 72 h at 27 °C in shaker flasks. Cells were harvested by centrifugation at 900 g for 10 min. The cell pellets were resuspended in PBS and pelleted again by centrifugation at 900 g for 20 min, then flash-frozen in liquid nitrogen and stored at -80 °C.

For mammalian expression, the same construct was also cloned into the pHTBV1.1-LIC baculovirus transfer vector (The BacMam vector backbone (pHTBV1.1), which was kindly provided by Professor Frederick Boyce, Massachusetts General Hospital, Cambridge, MA and adapted for ligation independent cloning in house) for expression in Expi293F cells (Thermo-Fisher Scientific, Cat. No. A14527). This vector also adds a TEV cleavable His10-FLAG tag to the C-terminus of the protein. For expression, 1 L of Expi293F cell cultures (2×10^6 cells/ml) in Freestyle 293™ Expression Medium (Thermo-Fisher) were transduced with 30 ml of P3 baculovirus (third passage) in the presence of 5 mM sodium butyrate in a 2 L roller bottle (Biofil). Cells were grown in a humidity controlled orbital shaker for 48 hours at 37 °C with 8% CO_2 before being harvested using the same process as for Sf9 cells.

Cell Lysis and detergent extraction of membrane proteins
Extraction Buffer (EXB): 50 mM HEPES-NaOH, pH 7.5, 500 mM NaCl, 5% v/v glycerol, 1 mM TCEP-NaOH, Roche protease inhibitor cocktail EDTA-free (1 tablet was used for 40 ml resuspended cells, dissolved in 1 ml Extraction buffer per tablet by vortexing prior to addition to the cell pellets).

Cell pellets were resuspended in EXB buffer (50 mM HEPES-NaOH, pH 7.5, 500 mM NaCl, 5% v/v glycerol, 1 mM TCEP-NaOH, Roche protease inhibitor cocktail EDTA-free) at the ratio of 50 ml per litre of equivalent original cell culture. The resuspension was then passed twice through an EmulsiFlex-C5 homogenizer (Avestin Inc.) at 10000 psi. Membrane proteins were extracted from the cell lysate with 1% w/v octyl glucose neopentyl glycol (OGNG; Generon, Cat. No. NG311) / 0.1% cholesteryl hemisuccinate tris salt (CHS; Sigma-Aldrich, Cat. No. C6512) and rotated for 2 h. Cell debris was removed by centrifugation at 35,000 x *g* for 1 h at 4 °C.

Purification
Wash Buffer: 50 mM HEPES-NaOH, pH 7.5, 500 mM NaCl, 1 mM TCEP-NaOH, 0.12% w/v OGNG / 0.012% w/v CHS and 20 mM imidazole pH 8.0

Elution Buffer: 50 mM HEPES-NaOH, pH 7.5, 500 mM NaCl, 1 mM TCEP-NaOH, 0.12% w/v OGNG / 0.012% w/v CHS and 250 mM imidazole pH 8.0

PD10 Buffer: 50 mM HEPES-NaOH, pH 7.5, 500 mM NaCl, 1 mM TCEP-NaOH, 0.15% w/v OGNG / 0.015% w/v CHS

Size exclusion buffer (SEC) Buffer: 20 mM HEPES-NaOH, pH 7.5, 200 mM NaCl, 1 mM TCEP-NaOH, 0.08% w/v OGNG/ 0.008% w/v CHS

Column 1: Co^{2+} TALON resin
The detergent-extracted supernatant was supplemented with 5 mM imidazole pH 8.0 before incubation with Co^{2+} charged TALON resin (Clontech) for 1 h on a rotator at 4 °C (1 ml resin slurry per L original culture volume). The Talon resin was collected by centrifugation at 700 x *g* for 5 mins and washed with 30 column volumes of wash buffer before the target protein was eluted with elution buffer. Peak fractions were combined and passed through PD10 columns, pre-equilibrated with four column volumes of PD10 buffer.

TEV protease cleavage and reverse purification
TEV protease was added at a ratio of 10:1 (ELOVL7:enzyme, wt:wt) and incubated at 4 °C overnight. For each litre of initial cell culture volume, 0.25 ml of a 50% slurry of TALON resin (pre-equilibrated as above) was

added and the sample was rotated at 4 °C for 1 hour. The sample was transferred to a gravity column and the flow-through was collected.

Column 2: Superdex 200 Increase 10/300 GL column (GE Healthcare)
The protein sample was concentrated in a 100 kDa MWCO Vivaspin 20 centrifugal concentrator (pre-equilibrated in SEC buffer without detergent) at 3,000 g, with mixing every 5 min, to a final volume of < 1 ml. After centrifugation at 21,000 g for 20 min at 4° C, the sample was subjected to size exclusion chromatography

Iodoacetamide modification
For structural studies, the flow through from the reverse Talon step was incubated with 50 mM iodoacetamide (IAM) (Merck Millipore) for 20 mins at room temperature. IAM was removed by passing the reaction mixture down a PD-10 desalting column prior to concentration. After SEC, fractions containing the highest concentration of ELOVL7 were pooled and concentrated to 12-25 mg/ml using a 100 kDa MWCO Vivaspin 20 centrifugal concentrator.

Crystallisation

Initial protein crystals were grown at 4 °C in condition E10 of the MemGold2-ECO Screen (Molecular Dimensions; 0.05 M Na-acetate pH 4.5, 0.23 M NaCl, 33 % v/v polyethylene glycol (PEG) 400) in 3-well sitting-drop crystallisation plates (SwissCi) with 150 nl drops and 2:1 and 1:1 protein to reservoir ratios. Crystals appeared after 4-7 days and grew to full size within 3-4 weeks. Two microlitre hanging drops were set up in 24-well XRL plates (Molecular Dimensions) at protein to reservoir ratios of 2.5:1, 2:1 and 1.5:1. The best crystals grew in 0.1 M Na-acetate pH 4.5, 0.23 M NaCl, 34-38% v/v PEG400 using the IAM-modified protein at a concentration of 5-8 mg/ml and were harvested after 12-14 days. Prior to vitrification, crystals were sequentially transferred to mother liquor solutions with an increasing amount of PEG400 to a final concentration of PEG400 of 46% v/v over 10-15 mins. For heavy atom derivatisation, crystals were looped into drops containing reservoir solution supplemented with 10 mM mercury chloride and soaked for 10 mins. Hg-soaked crystals were then treated to the same PEG400 escalation strategy using Hg-free solutions before being vitrified in liquid nitrogen. Diffraction data were collected at the I24 microfocus beamline at Diamond Light Source.

Structure Determination

ELOVL7 crystallises in monoclinic space group $P2_1$ with two copies of the enzyme in each asymmetric unit. All diffraction data were highly anisotropic and limited to between 3.4 - 4.5 Å resolution in the worse direction and 2.05 – 3 Å in the best direction. Phasing was carried out in PHENIX (22) using SIRAS with the Hg-peak data and a 3Å isomorphous lower resolution native dataset. Two Hg^{2+} sites were located with phenix.hyss using data to 4.5 Å (23). The resulting 3 Å phased electron density map had clear protein density allowing the identification of the NCS relationship between the two ELOVL7 molecules in the asymmetric unit. After two-fold averaging using RESOLVE, the resultant map was of sufficient quality to manually model all the TM helices. Initial phases were further improved by cross-crystal averaging with a non-isomorphous, less anisotropic and slightly higher resolution dataset using DMMULTI (24). The resultant map was of excellent quality and the majority of the structure could be built automatically with BUCCANEER (25). Model completion was carried out manually in COOT (26) and the structure was refined with BUSTER (27) using all data to 2.05 Å. The final model comprises residues 16-269 (chain B, 14-269), a covalently bound 3-keto-CoA acyl lipid, four OGNG detergent molecules and 112 solvent molecules.

Mass spectrometry

The denaturing intact mass spectrometry measurements were performed using an Agilent 1290 Infinity LC System in-line with an Agilent 6530 Accurate-Mass Q-TOF LC/MS (Agilent Technologies Inc.). The solvent system was consisted of 0.1% Optima™ LC/MS grade formic acid (Fisher Chemical) in HPLC electrochemical grade water (Fisher Chemical) (solvent A) and 0.1% formic acid in Optima™ LC/MS grade methanol (Fisher Chemical) (solvent B). Typically, 1-2 μg of protein sample was diluted to 60 μl with 30% methanol in 0.1%

formic acid. 60 μl of sample was injected onto a ZORBAX StableBond 300 C3 column (Agilent Technologies Inc.) by an auto sampler. The flowrate of the LC system was set to 0.5 ml/min. 30% of solvent B was applied in the beginning and the sample elution was initiated by a linear gradient from 30% to 95% of solvent B over 7 min. 95% B was then applied for 2 min, followed by 2 min equilibration with 30% B. The mass spectrometer was in positive ion, 2 GHz detector mode and spectra were recorded with capillary, fragmentor and collision cell voltages of 4000 V, 250 V and 0 V, respectively. The drying gas was supplied at 350°C with flow rate of 12 l/min and nebulizer at 60 psi. The data was acquired from 100-3200 m/z. Data analysis was performed using MassHunter Qualitative Analysis Version B.07.00 (Agilent) software.

In order to trap the covalent acyl-enzyme intermediate, the purified, tagged, wild-type ELOVL7 protein at 1.5 mg/mL (obtained after the desalting step that followed IMAC elution) was incubated with 100 μM C18:0-CoA (Avanti Polar Lipids, Cat. No. 870718) for 2 hours at 37 °C, in the presence and absence of 1 mM EDTA, 1 mM EGTA, or 100 μM Malonyl CoA (Sigma-Aldrich, Cat. No. M4263). The reaction was terminated by dilution into 30% methanol in 0.1% formic acid, as described above. Covalent acyl-enzyme intermediate formation was identified by monitoring the presence of a mass shift upon incubation with the substrate, corresponding to the addition of the substrate acyl chain through attachment of the histidine imidazole to the thioester carbonyl, resulting in thioester cleavage and loss of CoA (predicted +266.47 Da upon reaction with C18:0-CoA). The site of covalent modification was probed by carrying out this experiment with the His150Ala and His181Ala mutants, which allowed identification of His150 as the nucleophile involved in covalent intermediate formation.

References

1. Jakobsson, A., Westerberg, R., and Jacobsson, A. (2006) Fatty acid elongases in mammals: their regulation and roles in metabolism. *Prog Lipid Res* **45**, 237-249
2. Kihara, A. (2012) Very long-chain fatty acids: elongation, physiology and related disorders. *J Biochem* **152**, 387-395
3. Leonard, A. E., Pereira, S. L., Sprecher, H., and Huang, Y.-S. (2004) Elongation of long-chain fatty acids. *Progress in Lipid Research* **43**, 36-54
4. Ohno, Y., Suto, S., Yamanaka, M., Mizutani, Y., Mitsutake, S., Igarashi, Y., Sassa, T., and Kihara, A. (2010) ELOVL1 production of C24 acyl-CoAs is linked to C24 sphingolipid synthesis. *Proc Natl Acad Sci U S A* **107**, 18439-18444
5. Naganuma, T., Sato, Y., Sassa, T., Ohno, Y., and Kihara, A. (2011) Biochemical characterization of the very long-chain fatty acid elongase ELOVL7. *FEBS Lett* **585**, 3337-3341
6. Aldahmesh, M. A., Mohamed, J. Y., Alkuraya, H. S., Verma, I. C., Puri, R. D., Alaiya, A. A., Rizzo, W. B., and Alkuraya, F. S. (2011) Recessive mutations in ELOVL4 cause ichthyosis, intellectual disability, and spastic quadriplegia. *Am J Hum Genet* **89**, 745-750
7. Di Gregorio, E., Borroni, B., Giorgio, E., Lacerenza, D., Ferrero, M., Lo Buono, N., Ragusa, N., Mancini, C., Gaussen, M., Calcia, A., Mitro, N., Hoxha, E., Mura, I., Coviello, D. A., Moon, Y. A., Tesson, C., Vaula, G., Couarch, P., Orsi, L., Duregon, E., Papotti, M. G., Deleuze, J. F., Imbert, J., Costanzi, C., Padovani, A., Giunti, P., Maillet-Vioud, M., Durr, A., Brice, A., Tempia, F., Funaro, A., Boccone, L., Caruso, D., Stevanin, G., and Brusco, A. (2014) ELOVL5 mutations cause spinocerebellar ataxia 38. *Am J Hum Genet* **95**, 209-217
8. Westerberg, R., Tvrdik, P., Unden, A. B., Mansson, J. E., Norlen, L., Jakobsson, A., Holleran, W. H., Elias, P. M., Asadi, A., Flodby, P., Toftgard, R., Capecchi, M. R., and Jacobsson, A. (2004) Role for ELOVL3 and fatty acid chain length in development of hair and skin function. *J Biol Chem* **279**, 5621-5629
9. Moon, Y. A., Hammer, R. E., and Horton, J. D. (2009) Deletion of ELOVL5 leads to fatty liver through activation of SREBP-1c in mice. *J Lipid Res* **50**, 412-423
10. Matsuzaka, T., Shimano, H., Yahagi, N., Kato, T., Atsumi, A., Yamamoto, T., Inoue, N., Ishikawa, M., Okada, S., Ishigaki, N., Iwasaki, H., Iwasaki, Y., Karasawa, T., Kumadaki, S., Matsui, T., Sekiya, M., Ohashi, K., Hasty, A. H., Nakagawa, Y., Takahashi, A., Suzuki, H., Yatoh, S., Sone, H., Toyoshima, H., Osuga, J., and Yamada, N. (2007) Crucial role of a long-chain fatty acid elongase, Elovl6, in obesity-induced insulin resistance. *Nat Med* **13**, 1193-1202

11. Tolkach, Y., Merseburger, A., Herrmann, T., Kuczyk, M., Serth, J., and Imkamp, F. (2015) Signatures of Adverse Pathological Features, Androgen Insensitivity and Metastatic Potential in Prostate Cancer. *Anticancer Res* **35**, 5443-5451

12. Tamura, K., Makino, A., Hullin-Matsuda, F., Kobayashi, T., Furihata, M., Chung, S., Ashida, S., Miki, T., Fujioka, T., Shuin, T., Nakamura, Y., and Nakagawa, H. (2009) Novel lipogenic enzyme ELOVL7 is involved in prostate cancer growth through saturated long-chain fatty acid metabolism. *Cancer Res* **69**, 8133-8140

13. Li, G., Cui, S., Du, J., Liu, J., Zhang, P., Fu, Y., He, Y., Zhou, H., Ma, J., and Chen, S. (2018) Association of GALC, ZNF184, IL1R2 and ELOVL7 With Parkinson's Disease in Southern Chinese. *Front Aging Neurosci* **10**, 402

14. Parisi, L. R., Sowlati-Hashjin, S., Berhane, I. A., Galster, S. L., Carter, K. A., Lovell, J. F., Chemler, S. R., Karttunen, M., and Atilla-Gokcumen, G. E. (2019) Membrane Disruption by Very Long Chain Fatty Acids during Necroptosis. *ACS Chem Biol* **14**, 2286-2294

15. Ofman, R., Dijkstra, I. M., van Roermund, C. W., Burger, N., Turkenburg, M., van Cruchten, A., van Engen, C. E., Wanders, R. J., and Kemp, S. (2010) The role of ELOVL1 in very long-chain fatty acid homeostasis and X-linked adrenoleukodystrophy. *EMBO Mol Med* **2**, 90-97

16. Hernandez-Buquer, S., and Blacklock, B. J. (2013) Site-directed mutagenesis of a fatty acid elongase ELO-like condensing enzyme. *FEBS Lett* **587**, 3837-3842

17. Nie, L., Pike, A. C. W., Pascoa, T. C., Bushell, S. R., Quigley, A., Ruda, G. F., Chu, A., Cole, V., Speedman, D., Moreira, T., Shrestha, L., Mukhopadhyay, S. M. M., Burgess-Brown, N. A., Love, J. D., Brennan, P. E., and Carpenter, E. P. (2020) The structural basis of fatty acid elongation by the ELOVL elongases. *bioRxiv*, 2020.2011.2011.378570

18. Rizzo, W. B., Leshner, R. T., Odone, A., Dammann, A. L., Craft, D. A., Jensen, M. E., Jennings, S. S., Davis, S., Jaitly, R., and Sgro, J. A. (1989) Dietary erucic acid therapy for X-linked adrenoleukodystrophy. *Neurology* **39**, 1415-1422

19. Sassa, T., Wakashima, T., Ohno, Y., and Kihara, A. (2014) Lorenzo's oil inhibits ELOVL1 and lowers the level of sphingomyelin with a saturated very long-chain fatty acid. *J Lipid Res* **55**, 524-530

20. Morita, M., Honda, A., Kobayashi, A., Watanabe, Y., Watanabe, S., Kawaguchi, K., Takashima, S., Shimozawa, N., and Imanaka, T. (2018) Effect of Lorenzo's Oil on Hepatic Gene Expression and the Serum Fatty Acid Level in abcd1-Deficient Mice. *JIMD Rep* **38**, 67-74

21. Takamiya, M., Sakurai, M., Teranishi, F., Ikeda, T., Kamiyama, T., and Asai, A. (2016) Lead discovery for mammalian elongation of long chain fatty acids family 6 using a combination of high-throughput fluorescent-based assay and RapidFire mass spectrometry assay. *Biochem Biophys Res Commun* **480**, 721-726

22. Adams, P. D., Afonine, P. V., Bunkoczi, G., Chen, V. B., Davis, I. W., Echols, N., Headd, J. J., Hung, L. W., Kapral, G. J., Grosse-Kunstleve, R. W., McCoy, A. J., Moriarty, N. W., Oeffner, R., Read, R. J., Richardson, D. C., Richardson, J. S., Terwilliger, T. C., and Zwart, P. H. (2010) PHENIX: a comprehensive Python-based system for macromolecular structure solution. *Acta Crystallogr. D* **66**, 213-221

23. Wang, J. W., Chen, J. R., Gu, Y. X., Zheng, C. D., Jiang, F., Fan, H. F., Terwilliger, T. C., and Hao, Q. (2004) SAD phasing by combination of direct methods with the SOLVE/RESOLVE procedure. *Acta Crystallographica Section D* **60**, 1244-1253

24. Cowtan, K. D., Zhang, K. Y. J., and Main, P. (2012) *DM/DMMULTI software for phase improvement by density modification*, International Union of Crystallography

25. Cowtan, K. (2006) The Buccaneer software for automated model building. 1. Tracing protein chains. *Acta Crystallographica Section D* **62**, 1002-1011

26. Emsley, P., Lohkamp, B., Scott, W. G., and Cowtan, K. (2010) Features and development of Coot. *Acta Crystallogr. D* **66**, 486-501

27. Bricogne, G., Blanc, E., Brandl, M., Flensburg, C., Keller, P., Paciorek, W., Roversi, P., Sharff, A., Smart, O. S., Vonrhein, C., and Womack, T. O. (2017) BUSTER version 2.10.3. Global Phasing Ltd, Cambridge, UK

We respectfully request that this document is cited using the DOI value as given above if the content is used in your work.